

# Investigating the dependence of several surface plasmon characteristics on surrounding dielectric environment

LIU LU\*, XU ZHANG, XUAN TONG, NAIFEI REN, XIAOFANG XU, YU WU, YONG DING  
*School of Mechanical Engineering, Jiangsu University, Zhenjiang 212013, China*

Understanding the effect of dielectric environment around silver nanowires would be of great importance for their applications in surface plasmon (SP) mediated non-linear effects and plasmonic waveguide. In this paper, we investigate the dependence of several surface plasmon (SP) characteristics of silver nanowire, e.g. energy confinement, hot energy site, propagation length and coupling distance, on the surrounding dielectric environment. It is found that a homogeneous dielectric environment results in a uniform energy distribution around the surface of the nanowire, and a high dielectric environment contributes to stronger energy confinement and shorter propagation length. On the other hand, for an inhomogeneous dielectric environment, energy hot spots are observed closing to the surrounding material with largest refractive index. Furthermore, the energy hot spots around silver nanowires get more confined in an abrupt change of dielectric environment. Besides, we find that the dielectric environment also affects the SP coupling distance of the two nanowires. Hence, the present simulation results can provide valuable reference for the researches of SP assisted spectrum enhancement or plasmonic waveguide.

(Received September 13, 2014; accepted September 9, 2015)

*Keywords:* Surface plasmon, Nanowire, Dielectric environment, Electromagnetic field

## 1. Introduction

Surface plasmon resonance (SPR) is well known as one of the characteristic properties of noble metal nanostructure. Besides the morphology and dielectric properties of the metal nanostructures themselves, the SPR are also dependent on the dielectric environment where the metal structures are immersed [1]. Up to now, most of the research on the sensitivity of SPR to the dielectric environment concentrates on the surface Plasmon (SP) resonance frequency and SP dependent spectrum enhancement factor [2-5], [6-8]. However, for the SP applications in spectrum enhancement, sensors and nanowaveguide, other properties of SP, including the SP energy distribution, hot spot site, energy confinement and propagation length, are also critically important [9-14]. For example, compared to the SP resonance frequency, the SP enhanced spectrum are more sensitivity relies on hot spot of SP energy around the nanostructures [9-12]. The performances of various plasmonic waveguide are determined by the characteristics of SP field confinement and propagation length [13]. In addition, as an SP optical cavity, one can quantify the interaction between matter and the cavity using the quality factor  $Q$  and effective mode area  $A_{eff}$ , which depend on the SP energy confinement and losses [14]. Recently, the importance of the dielectric environment of the metal nanostructure has again attracts attentions [15-19]. It is found that careful control of the dielectric material properties adjacent to a metal can manipulate the SPs propagation in a prescribed transformative manner [16]. The dielectric loaded in SP waveguide has stronger confinement and less edge-scattering losses than that of bare metallic stripe

waveguide. And this type of SP waveguide can be used for the development of active plasmonic components [20-22].

All of the above phenomena motivate the requirement for theory that can describe the factors of SP energy distribution, hot spot site, confinement and propagation length of metal nanostructures subject to a complex external dielectric environment. Silver nanowire, supporting both of localized and propagating surface plasmons, is one of the promising nanostructures in the applications of plasmonic waveguide, cavity quantum electrodynamics, and spectrum enhancement [23-25]. Here, though adopting finite element method, we investigate the variations of several important characteristics of SP, e.g. field distribution, hot spot site, energy confinement, and SP propagation length, upon the change of the refractive index of matter close to the silver nanowire, with the goal of discovering principles that can predict the properties of SP in the actual application.

## 2. Simulation and results

As illustrated in Fig. 1, we consider the physical models of a single nanowire and two coupled nanowires imbedded in homogeneous and inhomogeneous medium. The model of Fig. 1(a) shows a single silver nanowire is totally imbedded in a homogeneous medium with refractive index  $n$ , while the model of Fig. 1(b) consists of single silver nanowire placed on glass substrate and covered with another material. The models shown in Fig. 1(c) and (d) are considering two coupled nanowires with a gap distance  $d$ . The diameter of silver nanowire in all models described in this work is 150 nm. The numerical simulation of SP filed

distribution and the related parameters was implemented using the commercial software of with the 2D electromagnetic wave module. The scattering boundary condition was used and the simulated region is 10  $\mu\text{m}$ \*10  $\mu\text{m}$ . A fixed wavelength of 637 nm circle light was used. As known, the surface plasmon resonance is induced by collective coherent excitations of the free finite element method (COMSOL Multiphysics 4.2a) electrons in silver nanowire under the irradiation of light, with a strong local EM field distributing around the surface.

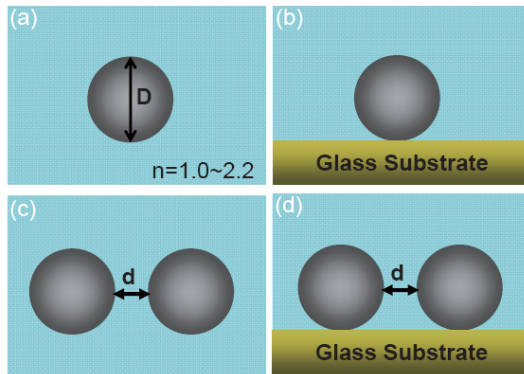


Fig. 1. The cross-sections of physical models for single nanowire and two coupled nanowires. A silver nanowire with the diameter  $D$  is (a) imbedded in homogeneous medium or (b) placed on glass substrate and covered by another dielectric material. The refractive index of the material is  $n$ . The cases of (c) and (d) are two coupled silver nanowire with gap distance  $d$ . A circle of light is used in the models.

Besides the local field distribution, the parameters of propagation length  $L$  and mode area  $A_{eff}$  are also very important for SP mode[13, 26]. As it is known, the SP mode would propagate harmonically along the nanowire, and the propagation length  $L$  is governed by the modal loss and is defined as the distance where the traveling wave power magnitude decays by  $1/e$ ,

$$L = \lambda / 4\pi \text{Im}(n_{eff}) \quad (1)$$

where the  $n_{eff}$  is the effective index of the mode. Another important parameter of the effective mode area  $A_{eff}$  can be set as the ratio of a mode's total energy density per unit length and its peak energy density,

$$A_{eff} = \int_{all} w(r) ds / \max[w(r)] \quad (2)$$

where  $w(r)$  is the energy density.

## 2.1. The effect of a homogeneous dielectric environment on the SP energy confinement.

One of the most attractive aspects of a silver nanowire is that it can be used as a plasmonic waveguide, in which they help us to guide and concentrate light in deep sub-wavelength confinement beyond the diffraction limit [23, 27]. The merits of a SP waveguide can be characterized via the concept of propagation length  $L$  and light confinement ability. In order to investigate the effect of the dielectric environment on the energy distribution of SP field and the above referred parameters, we first numerically simulate the SP local EM field distribution of a silver nanowire imbedded in a homogeneous medium, as shown in Fig. 2(a). The dependences of the effective index  $n_{eff}$ , mode area  $A_{eff}$  and propagation length  $L$  on  $n$  are also given in Fig. 2(b)–(d). As clearly observed from Fig. 2(a), with the increasing of  $n$ , the SP energy covering area becomes narrower, resulting in a stronger energy confinement. Thus, it indicates that a high dielectric environment would support a deeper sub-wavelength light confinement. This finding is important for the research of highly confinement of light in nanoscale, and particularly for the SP nano-waveguide. This result is also statistically demonstrated in Fig. 2(b) and (c), which show that the effective index  $n_{eff}$  and the mode area  $A_{eff}$  increases and decreases with the refractive index  $n$ , respectively. It is known that the parameter of  $A_{eff}$  describe the ability of energy confinement. Moreover, the smaller of the  $A_{eff}$  becomes, the more confined of the SP energy get. As shown in Fig. 2(c), the  $A_{eff}$  gets smallest for  $n=2.2$ , agreeing with the energy distribution profiles in Fig. 2(a). Besides the confinement ability, achieving a high propagation length  $L$  of SP mode is also a key goal for guiding light in SP assisted nano-waveguide. As illustrated in Fig. 2(d), it is clear indicated that the propagation length  $L$  reaches maximum and minimum for  $n=1.45$  and  $2.2$ , respectively. In fact, such a phenomenon is contributed by the trade-off between energy confinement and propagation distance [23,27].

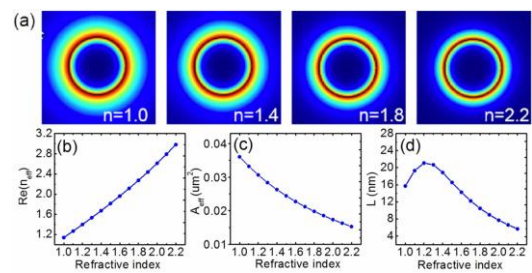


Fig. 2. (a) Field distribution plots for the model in Fig 1(a). The parameters of (b) effective index  $n_{eff}$  (c) propagation length  $L$  and (d) mode area  $A_{eff}$  of SP modes are plotted against the refractive index  $n$  of the coating material.

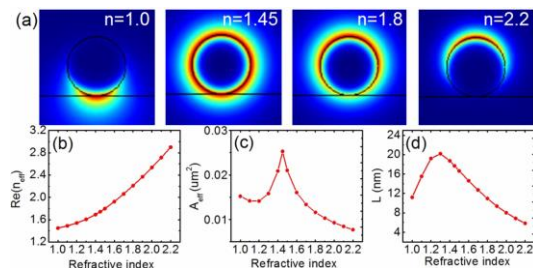


Fig. 3. (a) Field distribution plots for the model in Fig 1(b). The parameters of (b) effective index  $n_{eff}$ , (c) mode area  $A_{eff}$  and (d) propagation length  $L$  of SP modes are depicted as a function of the refractive index  $n$  of the covering materials

## 2.2. The effect of inhomogeneous dielectric environment on the SP energy distribution and the position of energy hot spot

In order to investigate the case of inhomogeneous dielectric environment, the silver nanowire is placed on glass substrate and covered by another material of the refractive index  $n$ , which is altered from 1.0 to 2.2. Fig. 3(a) compares the field distribution plots around the surface of silver nanowire for  $n=1.0, 1.45, 1.8$  and  $2.2$ . It can be clearly observed that, when  $n$  changes to 1.45, equal to that of the substrate, the distribution of EM field shows uniform and rotation symmetry around the nanowire, with a loosely confinement. However, as the  $n$  is 1.0 or 2.2, which is away from that of the substrate, the field distribution becomes non-uniform around the nanowire with an obvious energy hot spot. Thus the results in Fig 3(a) confirm that whether the SP energy distribution is uniform not only relies on the metal structure itself, but also on the distribution of the surrounding dielectric environment.

Moreover, Fig. 3(a) also indicates that an inhomogeneous dielectric environment would contribute to the generation of energy hot spot, and moreover, this energy hot spot gets more confined as the refractive index gap between the substrate and the upper material is large. Besides, another important phenomenon can also be revealed in Fig. 3a by comparative study of the cases  $n=1.0$  and  $2.2$ . For  $n=1.0$ , it is evident that most of the SP energy is confined in the silver-substrate interface and penetrated into the substrate. However, as the  $n$  is increased to 2.2, the confined energy is gradually extracted from the substrate, and finally focused on the top of silver-medium interface. This result reveals that the hot spots of SP local field always focus on the surface of metal, where the adjacent material has largest refractive index important for the coupling of emitter and SP energy, thus the above finding is very useful. There is another phenomenon that should be pointed out. Compared to that of  $n=1.0$ , the case of  $n=2.2$  has a larger gap of dielectric distribution, however, the energy confinement for  $n=1.0$  is larger. This phenomenon is attributed to that the covering area for  $n=2.2$  is larger. Furthermore, compared to that of  $n=1.0$ , the case of  $n=2.2$

with the hot site of the energy above the substrate is relatively easier for the sufficient use of the SP energy. It should be pointed out that to get the exact position of hot spot of local field is important for the coupling of emitter and SP energy, thus the above finding is very useful.

Fig. 3(b)-(d) illustrates the parameters of  $n_{eff}$ ,  $A_{eff}$  and  $L$  versus the refractive index  $n$  of the covering material. It shows that the  $n_{eff}$  increases with the refractive index, while the parameters of  $A_{eff}$  and  $L$  present a turning point as the  $n$  approaches the refractive index of the substrate. It is evident from Fig. 3(c) that the  $A_{eff}$  shows maximum and minimum for  $n=1.45$  and  $n=2.2$ , respectively, this result is consistent with the energy confinement shown in Fig. 3(a). The change of  $L$  with the  $n$  is plotted in Fig. 3(d). It is clear that the  $L$  first increases from 13 to 21  $\mu m$  as the  $n$  increases from 1.0 to 1.45, then drops to 7  $\mu m$  for  $n=2.2$ . The largest propagation length obtained at  $n=1.45$  is expected to be at the expense of confinement effect. Therefore, a homogenous dielectric environment around the nanowire is conducive to the design of SP waveguide with a larger propagation length  $L$ , while the inhomogeneous case is benefit for the energy hot spot. In fact, this finding can explain the physical origin of some experimental phenomena. For example, the silica-coated silver nanowire shows superior propagation length than the bare nanowire on substrate [28].

## 2.3. The effect of the surrounding dielectric environment on the SP coupling between two nanowires

The understanding of the interactions between strongly coupled metallic nanostructures has greatly matured in the past decade. Owing to the electromagnetics coupling field, two coupled nanowires can provide hot spots of EM field, light up more SP resonance, and act as an antenna to control the radiation direction of nearby molecule [29, 30]. The dielectric environment is also supposed to influence the electromagnetics coupling field of two nanowires. In this work, resonant SP coupling is achieved by placing two nanowires in close proximity. We compare the field distribution plots of two coupled silver nanowires imbedded in different material with  $n=1.0, 1.45$  and  $2.2$ , as shown in Fig. 4. The gap separation distance  $d$  between the two nanowires is set as 25, 50, 75 and 100 nm. With the increasing of the  $n$ , the coupling effect becomes weaker, and this phenomenon is more obvious for a larger distance gap. We attribute this phenomenon to the high refractive index induced stronger energy confinement. Moreover, in detail, from the field profile of  $d=100$  nm, the coupling originally existed in the cases of  $n=1.0$  and  $n=1.45$  almost disappears in the case of  $n=2.2$ . To get a deeper insight of the field coupling, Fig. 5 shows the energy densities along the centers of two coupled nanowires. From Fig. 5, it is clear that the intensity of the energy density on the nanowire's surface for  $n=2.2$  is strongest, however, it decreases with a sharpest rapid along the gap-center. As a result, at the gap-center for  $n=2.2$  and  $d=100$  nm, the energy becomes smallest with no coupling. The energy of

hot spot for  $n=1.1$  is almost 4 times as large as that of  $n=2.2$ . Therefore, both Fig. 4 and Fig. 5 account for that the dielectric environment affects the maximum coupling distance, and a high refractive index would result in a short maximum coupling distance.

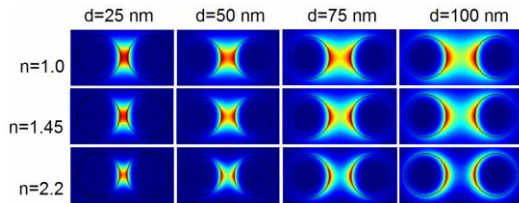


Fig. 4. Field distribution plots of two coupled silver nanowires totally imbedded in different medium with refractive index  $n$ . The parameter  $d$  is the distance of the gap separation between the two nanowires.

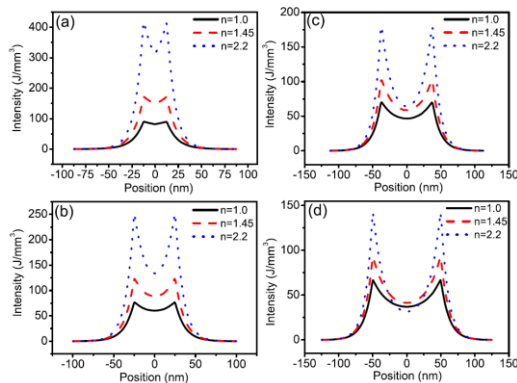


Fig. 5. (a)-(d) are the calculated energy densities along the centers of two coupled nanowires shown in Fig. 4 with different gap distances of 25, 50, 75 and 100 nm, respectively. The center between the two nanowires is set as 0 nm of the  $x$  axis.

As illustrated in Fig. 6, we also investigate the case for the two coupled silver nanowires in an inhomogeneous dielectric environment. The obtained most important result is that the original hot energy site in the gap of the two nanowires, is challenged by the energy-pull of the dielectric material with high refractive. For example, for the case of  $n=1.0$ , the SP coupling for  $d=25$  nm between the two nanowires dominates over the energy-pull of the glass substrate ( $n=1.45$ ). However, as the gap distance  $d$  is larger than 50 nm, the hot energy pulled by the substrate gradually becomes dominant. As the  $d$  further increases to 75 and 100 nm, the SP coupling almost thoroughly disappears. For  $n=2.2$  and  $d=100$  nm, because of the hot energy pulled by the covering material, the hot site is not in the center between the two nanowires. Nevertheless, in the case of the homogeneous dielectric environment shown in Fig.4, the SP coupling is still present for  $d=75$  and 100 nm. Therefore, it confirms that the dielectric environment around the nanowire also affects the SP coupling distance.

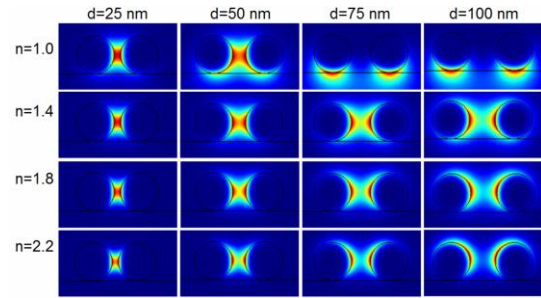


Fig. 6. Field distribution plots of two coupled silver nanowire on glass substrate. The parameter of  $n$  is the refractive index of the covering material on nanowires.

### 3. Conclusion

In conclusion, we study the variation of several SP characteristics, e.g. energy confinement, hot energy site, propagation and coupling of silver nanowire, upon the change of the surrounding dielectric environment. The results show that the uniformity of the field around the nanowire is dependent on the homogeneous feature of the surrounding dielectric environment. For a homogeneous dielectric environment, the SP energy exhibits rotation symmetry, and the properties of energy confinement and propagation length depend on the value of the refractive index of dielectric material. For an inhomogeneous dielectric environment, hot energy spots are brought and focused near the material with larger refractive index. The simulation results of two coupled nanowires demonstrate that both the distribution and the refractive index of the surrounding dielectric material affect the SP coupling distance.

### Acknowledgments

This work was funded by the National Natural Science Foundation of China (No. 21106058 and 11204107), China Postdoctoral Science Foundation (No. 2012M521005 and 2015M571678), National Basic Research Program of China (No. 2011CB013004) and Research Fund for Advanced Talents of Jiangsu University (Grants No. 1281110026). Open project of Jiangsu Province Key Laboratory of photon manufacturing science and technology (GZ201210)

### References

- [1] K. L. Kelly, E. Coronado, L. L. Zhao, G. C. Schatz, *Journal of Physical Chemistry B*, **3**, 668 (2003).
- [2] M. A. Mahmoud, M. Chamanzar, A. Adibi, M. A. El-Sayed, *Journal of the American Chemical Society*, **14**, 6434 (2012).
- [3] Y. Y. Li, J. Pan, P. Zhan, S. N. Zhu, N. B. Ming, Z. L. Wang, W. D. Han, X. Y. Jiang, J. Zi, *Optics Express*, **4**, 3546 (2010).
- [4] M. M. Miller, A. A. Lazarides, *Journal of Physical Chemistry B*, **46**, 21556 (2005).
- [5] M. D. Malinsky, K. L. Kelly, G. C. Schatz, R. P. Van



- Duyn, *Journal of Physical Chemistry B*, **12**, 2343 (2001).
- [6] S. Funke, H. Wackerbarth, *Journal of Raman Spectroscopy*, **7**, 1010 (2013).
- [7] E. C. Le Ru, E. Blackie, M. Meyer, P. G. Etchegoin, *Journal of Physical Chemistry C*, **37** 13794 (2007).
- [8] Y. C. Lu, Y. S. Chen, F. J. Tsai, J. Y. Wang, C. H. Lin, C. Y. Chen, Y. W. Kiang, C. C. Yang, *Applied Physics Letters*, **23**, 233113 (2009).
- [9] L. Lu, X. L. Xu, C. S. Shi, H. Ming, *Thin Solid Films*, **12**, 3250 (2010).
- [10] R. Chikkaraddy, D. Singh, G. V. P. Kumar, *Applied Physics Letters*, **4**, 043108 (2012).
- [11] K. Fukami, M. L. Chourou, R. Miyagawa, A. M. Noval, T. Sakka, M. Manso-Silvan, R. J. Martin-Palma, Y. H. Ogata, *Materials*, **4**, 791 (2011).
- [12] P. H. C. Camargo, C. M. Cobley, M. Rycenga, Y. N. Xia, *Nanotechnology*, **43**, 434020 (2009).
- [13] R. F. Oulton, G. Bartal, D. F. P. Pile, X. Zhang, *New Journal of Physics*, **10**, 105018 (2008).
- [14] S. A. Maier, *Optics Express*, **5**, 1957 (2006).
- [15] C. L. Zou, F. W. Sun, Y. F. Xiao, C. H. Dong, X. D. Chen, J. M. Cui, Q. Gong, Z. F. Han, G. C. Guo, *Applied Physics Letters*, **18**, 183102 (2010).
- [16] Y. M. Liu, T. Zentgraf, G. Bartal, X. Zhang, *Nano Letters*, **6**, 1991 (2010).
- [17] M. M. Miller, A. A. Lazarides, *The Journal of Physical Chemistry B*, **46**, 21556 (2005).
- [18] Y. H. Lai, P. M. Hui, *Optics Communications*, **304**, 111 (2013).
- [19] P. Bhatia, B. D. Gupta, *Photonics 2010: Tenth International Conference on Fiber Optics and Photonics*, **8173**, 111 (2011).
- [20] A. Krishnan, C. J. Regan, L. G. de Peralta, A. A. Bernussi, *Applied Physics Letters*, **23**, 231110 (2010).
- [21] J. Grandidier, G. C. des Francs, S. Massenot, A. Bouhelier, L. Markey, J. C. Weeber, C. Finot, A. Dereux, *Nano Letters*, **8**, 2935 (2009).
- [22] J. Grandidier, G. C. des Francs, L. Markey, A. Bouhelier, S. Massenot, J. C. Weeber, A. Dereux, *Applied Physics Letters*, **96**, 063105 (2010).
- [23] C. H. Dong, X. F. Ren, R. Yang, J. Y. Duan, J. G. Guan, G. C. Guo, G. P. Guo, *Applied Physics Letters*, **22**, 221109 (2009).
- [24] A. V. Akimov, A. Mukherjee, C. L. Yu, D. E. Chang, A. S. Zibrov, P. R. Hemmer, H. Park, M. D. Lukin, *Nature*, **7168**, 402 (2007).
- [25] Y. C. Wang, C. T. Yuan, M. Y. Kuo, M. C. Wu, J. Tang, M. H. Shih, *Applied Physics Letters*, **25**, 253110 (2012).
- [26] J. Chen, G. A. Smolyakov, S. R. J. Brueck, *Optics Express*, **19**, 14902 (2008).
- [27] X. Xiong, C. L. Zou, X. F. Ren, A. P. Liu, *Laser Photonics Review*, **7**, 901 (2013).
- [28] L. L. Wang, C. L. Zou, X. F. Ren, A. P. Liu, L. Lv, Y. J. Cai, F. W. Sun, G. C. Guo, *Applied Physics Letters*, **6**, 061103 (2011).
- [29] M. Davies, A. Wochnik, F. Feil, C. Jung, C. Brauchle, C. Scheu, J. Michaelis, *Acs Nano*, **7**, 6049 (2012).
- [30] L. Novotny, N. van Hulst, *Nature Photonics*, **2**, 83 (2011).

---

\*Corresponding author: lvliu@ujs.edu.cn